Microwave study of photoconductivity induced by laser pulses in rare-earth-doped dielectric crystals

M.-F. Joubert,[1] S. A. Kazanskii,[2] Y. Guyot,[1] J.-C. Gâcon,[1] and C. Pédrini[1]
[1]*LPCML, UMR 5620 CNRS, Université Claude Bernard Lyon 1, 10 rue A.M. Ampère, Domaine scientifique de la Doua, 69622 Villeurbanne Cedex, France*
[2]*S.I. Vavilov State Optical Institute, 12 Birzhevaya Line, 199034, St. Petersburg, Russia*
(Received 19 December 2003; published 29 April 2004)

Transient responses of the dielectric permittivity $\varepsilon=\varepsilon_1-i\varepsilon_2$ of rare-earth-doped dielectric crystals under pulsed laser excitation were studied by the 8-mm microwave resonator technique at room temperature. The fluorite-type crystals (CaF_2, SrF_2, and BaF_2) which contained divalent ions of Sm, Eu, and Tm, as well as $Lu_2(SiO_4)O$ and $Y_3Al_5O_{12}$ doped with trivalent Ce ions were investigated. The dielectric response to a laser pulse contains two different types of signals: electronic and heating ones. The electronic peak, which is quite fast (from 40 to 100 ns or more), is the signature of electrons released into the conduction band following an impurity photoionization. The prolonged heating signal has a sawtooth form on which oscillations are imposed. It is due to modulation of the dielectric constant by a sudden temperature rise and subsequent elastic vibrations of the sample caused by the energy absorbed from the laser pulse. In different crystals the electronic peak was caused by the transient response of either ε_1, ε_2, or a mixture of the two. The modulation of the dielectric loss factor ε_2 corresponds to conventional photoconductivity, i.e., the photoexcitation of mobile electrons. The modulation of the dielectric constant ε_1 corresponds to the photoexcitation of ''bound'' electrons, probably captured by traps. The threshold energies of photons at which the photoionization of rare-earth ions may occur, were determined for $CaF_2:Sm^{2+}$ (3.3 eV) and $Lu_2(SiO_4)O:Ce^{3+}$ (3.1 eV). In fluorite-type crystals doped with Sm^{2+} or Tm^{2+} ions, the significant reduction of a lifetime of electrons in a conduction band was revealed with an increase in energy of laser pulses. In $SrF_2:Eu$ crystal the record-high signals of ''photoconductivity'' were observed upon excitation by VIS light in the optical region of ''transparency'' of this crystal. The microwave resonant technique may be used for detail studying the photoionization dynamics of rare-earth ions and finding the location of their energy levels with respect to the host conduction band in doped insulators.

DOI: 10.1103/PhysRevB.69.165217 PACS number(s): 78.20.−e

I. INTRODUCTION

It is well known that high-energy excitations (with UV, VUV, x, or even γ rays) of rare-earth (RE) ions embedded in a wide-band-gap crystalline material can lead to ionization of impurities and delocalization of electrons. So, to control excitation and emission mechanisms in luminescent materials (for mercury-free fluorescent tubes, plasma display panels, VUV detectors in wafer steppers, fast scintillators, tunable UV or VUV lasers, etc.), it is necessary to study the quantum efficiency of the RE ion photoionization process, the lifetime and mobility of photoexcited electrons, as well as the location of the RE energy levels within the forbidden band gap.

Various experimental approaches have been applied in the past to measure the energy gap either between the valence band and the rare-earth ion ground state (E_{vg}), or between the rare-earth ion ground state and the conduction band (E_{gc}) of crystals. For E_{vg} evaluation, conventional x-ray or UV photoelectron spectroscopy (XPS or UPS, respectively), which are based on kinetic energy measurement of emitted photoelectrons, can be used.[1] A resonant photoemission technique, combined with a refined and improved electrostatic point-charge model, was recently proved to be a more powerful tool; however, it needs a tunable VUV excitation source such as synchrotron radiation.[2] The main obstacle in applying these techniques is the large positive charge generated in the crystal by removing electrons, these charging effects being difficult to suppress or minimize. Furthermore, for activator ions at the beginning of the rare-earth series, which contain a small number of $4f$ electrons, a quite high concentration is necessary to carry out the measurement.[1–2] On the other hand, the energy gap E_{gc} between the rare-earth ion ground level and the bottom of the conduction band may be obtained *via* photocurrent measurements. However, in rare-earth doped insulating materials, the weakness of photocurrents to be detected (typically between 10^{-12}–10^{-16} A/cm^2) and polarization problems due to the use of blocking contacts make measurements very delicate.[3,4]

For the detailed study of the rare-earth ion photoionization and determining E_{gc} in RE-doped insulators, a microwave resonator technique might be used. This ''contactless'' technique should be able to detect the dielectric response of a rare-earth doped crystal inserted in a resonant microwave cavity and irradiated by photons of sufficient energy to induce the rare-earth photoionization. The first results of photoconductivity measurements with this microwave method in dielectric crystals were recently reported in Ref. 5. Previously, microwave measurements of photoconductivity were performed for crystals possessing semiconducting properties.[6–9] For dielectric crystals, however, observable signals are supposed to be considerably smaller than those for semiconductors. So, in this case it is necessary to apply highly sensitive hardware developed for EPR experiments.[10]

In this work we applied such hardware for recording the

transient responses of the rare-earth-doped dielectric crystal permittivity under pulsed laser excitation of the RE ion $4f^{n-1}5d$ states. The resonator method of measurements with microwaves of $\lambda \approx 8$ mm was used. We investigated Sm-, Eu-, and Tm-doped fluorite-type crystals for which ''photoactive'' $4f^{n-1}5d$ absorption bands are located in the near infrared, visible or near ultraviolet spectral range,[4] which are easily accessible with tunable lasers. We also investigated two scintillator crystals: $Lu_2(SiO_4)O:Ce^{3+}$ and $Y_3Al_5O_{12}:Ce^{3+}$ in which the Ce^{3+} ion photoionization threshold was previously evaluated at 3.1 eV (Refs. 11–12) and 3.8 eV,[4] respectively, by conventional photoconductivity measurements.

In Sec. II, the sensitivity of a microwave-resonator method is estimated and compared with that of a conventional photoconductivity method of measurement in a ''condenser with blocking electrodes.'' Section III is devoted to a detailed description of the experimental technique. In Secs. IV and V, experimental results are presented and discussed. Finally, Sec. VI contains brief conclusions of the work. In the paper, equations are expressed in the cgs (centimeter-gram-second) Gaussian system.

II. SENSITIVITY OF MICROWAVE RESONATOR TECHNIQUE

To estimate the sensitivity of a microwave-resonator method applied to photoconductivity measurements in dielectric crystals we can utilize the theory of EPR and easily rewrite it for the case of microwave absorption due to dielectric losses. We will restrict ourselves to the case of a reflex cavity and a linear microwave detector.[10,13] It follows that the sensitivity limit of the microwave technique to detect a change in the dielectric loss factor ε_2 of the sample is

$$(\Delta\varepsilon_2)_{\min}=\frac{2\varepsilon_1}{\eta Q_u}\left(\frac{k_B T_N df}{P_0}\right)^{1/2}, \tag{1}$$

where k_B is Boltzman's constant, T_N is the noise temperature of the microwave detector, Q_u is the unloaded quality factor of the reflex resonator, which takes into account the microwave power losses within the resonator with the sample and not the power leakage out of the cavity into the waveguide, P_0 is the microwave power dissipated in the resonator, and df is the bandwidth of the electronic circuit of the signal recording channel. ε_1 is the dielectric constant of the sample. η is the filling factor, which is equal to the ratio of the energy of the electrical component of the microwave field in the sample to that in the whole volume of the resonator. η value may be calculated for a given sample inside the resonator.[9] By an order of magnitude, η is about $\varepsilon_1 V_S/V_C$, where V_S and V_C are the volumes of the sample and the resonator correspondingly.[10] $\varepsilon_1=6.63$ for CaF_2, (Ref. 14) and the calculated value of η is about 0.4 for a ''standard'' sample of fluorite crystal of $d\approx 2.5$ mm diameter and $h\approx 2.5$ mm height, used in this work.[9] Assuming the parameter values $Q_u=2000$, $df=100$ MHz, $P_0=20$ mW, and $T_N=1000$ K, we obtain $(\Delta\varepsilon_2)_{\min}\sim 10^{-7}$.

Let us estimate the capacity of the microwave method for photoconductivity measurements upon pulsed laser excitation of dielectric crystals. If Θ is the quantum efficiency of an incident photon to generate a photoelectron and if such a free electron in the crystal conduction band has a mobility μ, the sensitivity of the technique can be estimated by the evaluation of $(\Theta\mu)_{\min}$, the minimum value for which photoconductivity is still detectable. Pulsed laser irradiation with average power P_{las}, repetition rate F, and pulse width τ_{las}, shorter than the lifetime τ_{el}, of the photoexcited electrons into the conduction band, causes an average number of electrons in the conduction band during the laser pulse equal to

$$\Theta\frac{P_{\text{las}}}{Fh\nu}, \tag{2}$$

where $h\nu$ is the energy of each photon of the laser beam. When the transient signal is accumulated and averaged after N laser pulses, from the expression $\sigma=ne\mu/V_S$ for conductivity,[15] in which n is the number of electrons in the sample of volume V_S and e is the electron charge, the minimum detectable change in the conductivity is

$$(\Delta\sigma)_{\min}=\frac{\sqrt{N}}{V_s}\frac{P_{\text{las}}}{Fh\nu}e(\Theta\mu)_{\min}. \tag{3}$$

So, combining Eqs. (1) and (3), the minimum detectable photoconductivity is

$$(\Theta\mu)_{\min}=\frac{Fh\nu}{eP_{\text{las}}\sqrt{N}}\frac{V_s f_0\varepsilon_1}{\eta Q_u}\sqrt{\frac{k_B T_N df}{P_0}}. \tag{4}$$

For its numerical estimation, we use the central frequency of the cavity $f_0=35$ GHz and we assume $\tau_{\text{el}}=10^{-7}$ s. For laser pulses of wavelength 355 nm, $\tau_{\text{las}}\sim 10^{-8}$ s, $P_{\text{las}}=10$ mW, and $F=10$ Hz and taking for the other parameters the same values as before, we get $(\Theta\mu)_{\min}=4\times 10^{-8}$ cm^2 V^{-1} s^{-1} after $N=10$ laser pulses, i.e., for 1 s of signal accumulation. Note, that with an increase in accumulation time, the sensitivity will grow as $\sim\sqrt{N}$.

Let us estimate the most effective conventional method for studying photoconductivity of the same dielectric crystals ''in condenser with blocking electrodes.'' [3–4,16–18] In those experiments, a voltage U is applied to the condenser plates and the ''leakage'' current I through them is measured, upon illumination of the crystal inside the condenser by photons of energy $h\nu$. If P_l is the luminous power reaching the crystal and if τ_{el} is the lifetime of photoexcited electrons into the conduction band, the average number of electrons promoted into the conduction band is

$$\frac{P_l}{h\nu}\tau_{\text{el}}\Theta, \tag{5}$$

and the conductivity is

TABLE I. Experimental parameters of the studied crystals.

Sample	h (cm)	RE content (mol. %)	RE^{2+} content (mol. %)[d]	green light ($\lambda=532$ nm)			UV light ($\lambda=355$ nm)			
				k (cm^{-1})	S^{el} (V)[a]	S^{ht} (V)[a]	k (cm^{-1})	S^{el} (V)[a]	S^{ht} (V)[a]	$S^{el}_{abs}/S^{el}_{dis}$
LSO:Ce^{3+}	1.0	0.11[c]	0	<0.03	0	0.04	32	2.0	0.1	1/0
YAG:Ce^{3+}	0.25	0.89[c]	0	0.037	0.2	0	5.0	0.8	0.25	
CaF_2:Eu	0.215	0.01[b]	0.009				12	0.5	0.5	1/0
SrF_2:Eu	0.235	0.5[b]	0.04	<0.05	3.0	0	~ 60	0.4	0.3	
CaF_2:Sm (No. 1)	0.25	0.19[c]	0.02	2.3	0	0.6	2.1	0.3	0.6	0.5/0.5
CaF_2:Sm (No. 2)	0.25	0.15[c]	0.006	0.68	0	0.2	1.4	0.2	0.1	
SrF_2:Sm (No. 1)	0.15	0.21[c]	0.04	6.6	0.6	$\leqslant 0.1$	6.3	1.5	$\leqslant 0.1$	0/1
SrF_2:Sm (No. 2)	0.155	0.17[c]	0.01	1.9	0.04	0.25	1.6	0.25	0.15	
SrF_2:Sm (No. 3)	0.225	~ 0.1[b]	0.004	0.80	0.02	0.15	0.82	0.2	0.1	
CaF_2:Tm	0.25	0.2[b]	0.002	0.34	0.04	0.04	0.52	0.25	0.04	
SrF_2:Tm	0.25	~ 0.5[b]	0.005	0.69	0.02	0.2	0.42	0.15	0.1	
BaF_2:Tm	0.25	~ 0.5[b]	0.0005	0.15	0.05	0.1	0.30	0.7	0.15	

[a]Signal amplitudes measured under laser pulses of 1 mJ energy.
[b]Concentration in the batch.
[c]Concentration measured by chemical analysis.
[d]Concentration evaluated by absorption measurements.

$$\sigma = \frac{P_l}{h\nu}\tau_{el}\Theta\frac{e\mu}{V_s}. \tag{6}$$

With hc the distance between the condenser plates, the minimum detectable current is then

$$I_{min} = \frac{P_l}{h\nu}\tau_{el}e(\Theta\mu)_{min}\frac{U}{h_c^2}. \tag{7}$$

In the case of a continuous light source, the sensitivity of the measurement is directly proportional to τ_{el}. Assuming $\tau_{el}=10^{-7}$ s and using the experimental numerical values of Refs. 4 and 5, i.e., $I_{min}=10^{-16}$ A, $P_l/h\nu \approx 10^{14}$ photons/s, $U\approx 10^3$ V, and $h_c \geqslant 1$ mm, we find that the photosensitivity parameter is equal to[19] $\tau_{el}(\Theta\mu)_{min} \geqslant 6\times 10^{-17}$ $cm^2\,V^{-1}$ and $(\Theta\mu)_{min} \geqslant 6\times 10^{-10}$ $cm^2\,V^{-1}\,s^{-1}$.

Thus, the microwave technique under discussion, has a sensitivity by about two orders of magnitude less than that of the conventional method of measurement in a ''condenser with blocking electrodes.'' However, the study of transient dielectric response of a crystal on pulses of laser light allows one to observe the development of the photoconductivity process in time. In addition, the sensitivity of microwave measurements can be increased by the prolonged accumulation of a signal with a digital oscilloscope from the large number N of pulses of a laser working in a periodic regime.

It should be noted that the microwave technique for studying ''stationary'' photoconductivity upon illumination of a crystal by light of continuous laser could not compete with the conventional method. Indeed the corresponding equation for the stationary microwave measurement is

$$(\Theta\mu)_{min} = \frac{h\nu}{eP\tau_{el}}\frac{V_s f_0 \varepsilon_1}{\eta Q_u}\sqrt{\frac{k_B T_N df}{P_0}}. \tag{8}$$

Assuming the accumulation of a signal during 1 sec ($df=1$ Hz), the $P=10$ mW power of a continuous laser and the same values of other parameters as above, we obtain: $\tau_{el}(\Theta\mu)_{min} \geqslant 10^{-12}$ $cm^2\,V^{-1}$ and $(\Theta\mu)_{min} \sim 10^{-5}$ $cm^2\,V^{-1}\,s^{-1}$. Thus, the sensitivity of a microwave technique using a continuous laser is of about two orders of magnitude less than that for a pulsed laser of the same mean power. The increase in a signal-to-noise ratio by a factor $\sim 10^4$ due to reduction in a frequency band of the detecting circuit at stationary microwave measurements does not make up for its decreasing by a factor τ_{el}^{-1} because of a short lifetime of the photoexcited carriers in the conduction band. The short and powerful pulse of light from a pulsed laser forms a ''package'' of electrons in the conduction band of a crystal, while much less intense light from a continuous laser creates the electrons continuously, but their time-independent concentration is less by a factor of $\sim \tau_{el}^{-1}$ than during the operation of the pulsed laser.

III. EXPERIMENTAL

In this work we studied Ca, Sr, and Ba fluoride crystals doped with Eu, Sm, and Tm ions, as well as $Lu_2(SiO_4)O:Ce^{3+}$ (LSO:Ce^{3+}) and $Y_3Al_5O_{12}:Ce^{3+}$ (YAG:Ce^{3+}) crystals with concentrations of RE ions varying from 0.01 to 0.9 mol. % (see Table I). As-grown fluorite-type crystals contained only trivalent Sm and Tm ions, and Eu ions both in divalent and trivalent state. To get a fraction of the samarium and thulium ions in the divalent state, these fluoride crystals were subjected to additive coloration.[20–22] Only CaF_2:Tm was colored by γ irradiation from a Co^{60} source.[23] However, most of the RE ions in fluoride crystals remained trivalent, except for CaF_2:Eu, see Table I. All crystal samples were cut and polished with random crystallographic orientation to cylindrical shape of $d\approx 2.5$ mm diam-

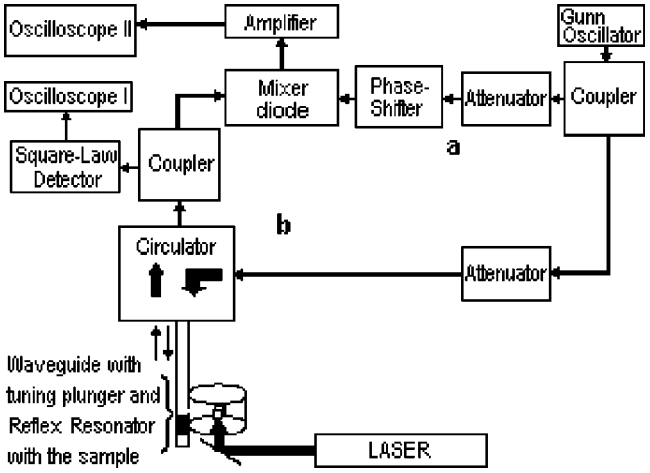

FIG. 1. Simplified block diagram of the experimental setup; (a) reference arm, (b) measuring arm. The resonator is shown with a sample inside. Oscilloscope I is used for monitoring the balance of the measuring channel. Oscilloscope II is used for recording the transient signal.

eter and various height from 0.8 to 10 mm.

The simplified block diagram of the experimental set-up is shown in Fig. 1. It was built on the basis of a homodyne microwave bridge used in EPR spectrometers. The microwave source was a ~ 50 mW Gunn oscillator with fixed operating frequency which could be manually adjusted in the range 35.3–35.7 GHz. The microwave power from this Gunn oscillator devides between a reference arm (a) and a measuring arm (b). In the reference arm, after an attenuator and a phase shifter, the microwave power goes to the reference input of a mixer diode. The mixer is a phase-sensitive linear detector,[10] for recording weak signals reaching its signal input from the measuring arm in phase with the microwaves at the reference input. The output voltage of a mixer is proportional to the amplitude of the electrical component of the incident microwave at its signal input. The measuring arm has a cylindrical reflex resonator operating in the TE_{011} mode. The inner diameter of the resonator cavity is ~ 12 mm. Its height can be adjusted from 5 to 10 mm by the pistons screwed in the top and bottom lids of the resonator. The crystal samples were fixed inside a thin-walled teflon tube which was put inside the resonator cavity through a hole in the upper piston of the resonator.

At first, the measuring arm of the microwave setup was balanced. The frequency of the Gunn oscillator was fixed to the central frequency of the resonator f_0. The match of the resonator with the waveguide was regulated with a tuning plunger at the end of the waveguide. Approximately complete matching of the resonator to the waveguide, $\beta \approx 1$ (see below), was achieved, so that the microwave power reaching the signal input of the mixer was nearly zero. This balance was monitored by a square-law detector which was fed through a coupler in the measuring arm. Then, the samples were irradiated by pulses of laser light through a hole in the bottom piston of the resonator.

Four different lasers with 10 Hz repetition rate and 15 ns pulse width were used. A frequency doubled or tripled Nd:YAG laser was used for fixed green ($\lambda = 532$ nm) or UV ($\lambda = 355$ nm) light generation. Spectral dependencies were obtained with an excimer (308 nm) pumped dye laser for wavelength generation between 350 and 410 nm and a pulsed Nd:YAG pumped OPO laser for wavelength generation between 460 and 670 nm. The frequency-doubled output beam from a pulsed Nd:YAG pumped tunable dye laser was also used for measuring spectral dependencies in the 275–420 nm wavelength range. In this case, BBO and KDP crystals were used for frequency doubling and it was necessary to realign the laser beam reaching the sample for each measurement.

The irradiation by laser pulses of a sample inserted in the resonator cavity resulted in a disbalance of the measuring arm and the occurrence of a transient signal reaching the detectors. The output signal from the mixer was amplified by a broadband amplifier with the high-frequency passband of 100 MHz and then visualized and averaged through a digital oscilloscope synchronized with the excitation laser. Usually, 300 pulses were taken for each measurement. The low-frequency passband of the amplifier was 1 MHz, resulting in some distortion of the waveform of ''slow'' signals. So, for recording such signals, another amplifier with a bandpass of 0.005–20 MHz was used. The experimental data discussed in Secs. IV and V are normalized to the same gain (1000) for both amplifiers. To eliminate the ''dragging'' pulse signals in time, we employed a resonator with a rather low unloaded quality factor Q_u, of about 2000. The transient time of electromagnetic field in the resonator was $\sim \tau_{\rm res} = Q_u / \pi f_0 (1 + \beta) \approx 9$ ns.

The signal in the measuring arm is formed upon reflection of microwaves from the reflex resonator with a sample. The complex reflection coefficient for the electrical component of the microwave field is given by[10]

$$R^E_{\rm refl}(f) = \frac{\overline{E}_{\rm refl}(f)}{\overline{E}_{\rm inc}} = \frac{\overline{z_R} - \overline{z_L}}{\overline{z_R} + \overline{z_L}} \approx \frac{1-\beta}{1+\beta} + i \frac{4\beta Q_u}{(1+\beta)^2} \frac{f - f_0}{f_0}, \tag{9}$$

where $\overline{E}_{\rm refl}$ and $\overline{E}_{\rm inc}$ are the complex amplitudes of the electric field of the reflected and incident waves, respectively, $\overline{z_R}$ and $\overline{z_L}$ are the complex characteristic impedances of the resonator and the waveguide, and β is the coupling coefficient of the resonator with the waveguide. The approximate equality on the right side of Eq. (9) holds for our measurements, which were carried out near the resonance frequency $f \approx f_0$. When the resonator is matched to the waveguide $\beta = 1$ and there is no reflected wave at the resonance frequency $\overline{E}_{\rm refl}(f = f_0) = 0$. Depending on the phase adjustment of the phase shifter in the reference arm, it was possible to continuously readjust the setup to record the real or imaginary parts of a reflected wave and to get the microwave signals in either absorption, dispersion, or mixed mode.

Using the relation

$$\delta\beta / \delta Q_u = \beta / Q_u, \tag{10}$$

we can find the signal in absorption mode near match, which corresponds to a change in the Q factor of the resonator by δQ_u:

$$S^E_{\rm abs} \sim |\overline{E}_{\rm inc}| \frac{\partial R^E_{\rm refl}(f=f_0,\beta,Q_u)}{\partial \beta} \beta \frac{\delta Q_u}{Q_u}$$

$$= -|\overline{E}_{\rm inc}| \frac{2\beta}{(1+\beta)^2} \frac{\delta Q_u}{Q_u}. \quad (11)$$

The signal in dispersion mode corresponds to a change in the central frequency of the resonator by δf:

$$S^E_{\rm dis} \sim |\overline{E}_{\rm inc}| \frac{\partial R^E_{\rm refl}(f,\beta,Q_u)}{\partial f} \delta f = i|\overline{E}_{\rm inc}| \frac{4\beta Q_u \delta f}{(1+\beta)^2 f_0}. \quad (12)$$

The amplitude of the recorded signal grows with an increase in the microwave power dissipated in the resonator. Therefore all the accessible power from Gunn oscillator was utilized in the experiments. However, most of the samples studied had dielectric losses and were warmed in the strong microwave field inside the resonator. The laser irradiation of the samples also caused their heating. When the samples were warmed, their dielectric constant was varied and, as a consequence, the central frequency of the resonator with the sample was shifted. Accordingly, it was necessary to adjust the frequency of Gunn oscillator. The settling time of a sample temperature after switching on both the microwave power, and the laser operating in a periodic regime was about 1 min. The frequency drift of the resonator with the sample during the experiment made it impossible the preliminary tuning of the setup to measure the signals exactly in absorption (or dispersion) mode with the mixer. However, the ''intense enough'' transient signals were recorded and their absorptive and dispersive parts evaluated with the square-law detector in the measuring arm of the setup, see Fig. 1. For a square-law detector the output voltage is proportional to the power of microwave at its input. For the microwave power, the frequency dependence of the reflection coefficient of the cavity is given by[10]

$$R^P_{\rm refl}(f) = \frac{P_{\rm refl}(f)}{P_{\rm inc}} = 1 - \frac{4\beta f_0^2}{(1+\beta)^2 f_0^2 + 4(f-f_0)^2 Q_u^2}, \quad (13)$$

where $P_{\rm inc}$ and $P_{\rm refl}$ are the microwave power incident and reflected from the resonator. For measurements with the square-law detector, we used the weak coupling: $\beta = 0.3$–0.5. The study of $R^P_{\rm refl}(f)$ dependence allows us to find experimental values of β and Q_u, using the relations $R^P_{\rm refl}(f=f_0) = [(1-\beta)/(1+\beta)]^2$ and $Q_u = (1+\beta)(f_0/\Delta)$, where Δ is the full-width at half maximum of the $R^P_{\rm refl}(f)$ dependence, see Fig. 2. The laser irradiation of the sample inside the cavity might result in a change in both the resonant frequency of the cavity by δf (dispersion mode) and the Q factor by δQ_u (absorption mode). If these effects persist long enough after a laser pulse (in the case of $\tau_{\rm el} \geqslant \tau_{\rm las} \geqslant \tau_{\rm res}$), the frequency dependence of the recorded signal with the square-law detector is given by

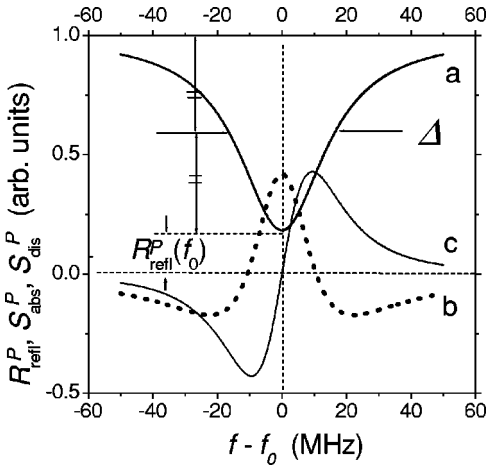

FIG. 2. (a) Calculated frequency dependence of the reflection coefficient $R^P_{\rm refl}$ of the reflex cavity in the frequency range close to its resonance frequency f_0 for parameter values of $f_0 = 35$ GHz, $Q_u = 1500$, and $\beta = 0.4$. (b), (c) Calculated frequency dependencies of signals in absorption (b) and dispersion (c) mode when measured with a square-law microwave detector.

$$S^P_{\rm abs}(f) = \left(\beta \frac{\partial P_{\rm refl}(f,\beta,Q_u)}{\partial \beta} + Q_u \frac{\partial P_{\rm refl}(f,\beta,Q_u)}{\partial Q_u} \right) \frac{\delta Q_u}{Q_u} \quad (14)$$

for the ''pure'' absorption mode and

$$S^P_{\rm dis}(f) = \frac{\partial P_{\rm refl}(f)}{\partial f} \delta f \quad (15)$$

for the ''pure'' dispersion mode. The typical view of these two functions are presented in Fig. 2. Usually, the experimental signal was the mixture of the two. Its study makes it possible to extract the amplitude values of the signal in the absorption and dispersion modes and to determine the corresponding values of δQ_u and δf to an accuracy of $\pm 20\%$. In our case the recorded signal is the result of a change in the dielectric permittivity $\varepsilon = \varepsilon_1 - i\varepsilon_2$ of the sample irradiated by laser pulses inside the resonator. Having made the appropriate calculations,[9] using the experimental values of δf and δQ_u we may determine the corresponding changes in the dielectric constant $\Delta\varepsilon_1$ and the dielectric loss factor $\Delta\varepsilon_2$ of the sample under laser irradiation.

The experimental data on signal amplitudes presented and discussed in the next sections correspond to the definite changes in the dielectric permittivity of the samples. By an order of magnitude, the amplitude $S_{\rm abs} = 1$ V of the signal in absorption mode corresponds to the change in the Q factor of the resonator by $\delta Q_u/Q_u \sim -0.01$, and the amplitude $S_{\rm dis} = 1$ V of the signal in dispersion mode corresponds to the shift of the central frequency of the resonator by $\delta f \sim -0.1$ MHz. For ''standard'' cylindrical samples of doped fluorite-type crystals of 2.5 mm diameter and 2.5 mm height placed in the center of the resonator, signals in absorption and dispersion mode of 1 V amplitude correspond to the changes in real and imaginary parts of the permittivity ($\Delta\varepsilon_1$ and $\Delta\varepsilon_2$, respectively) by an order of magnitude of about 10^{-4}.

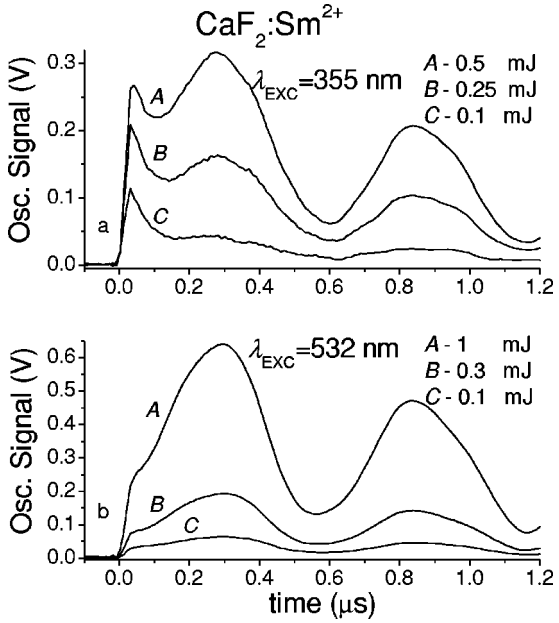

FIG. 3. Transient dielectric responses of $CaF_2:Sm$ (No. 1) crystal on laser pulses of (a) UV ($\lambda=355$ nm) light and (b) green ($\lambda=532$ nm) light of different energy: (a) $A-0.5$ mJ, $B-0.25$ mJ, and $C-0.1$ mJ; (b) $A-1$ mJ, $B-0.3$ mJ, and $C-0.1$ mJ.

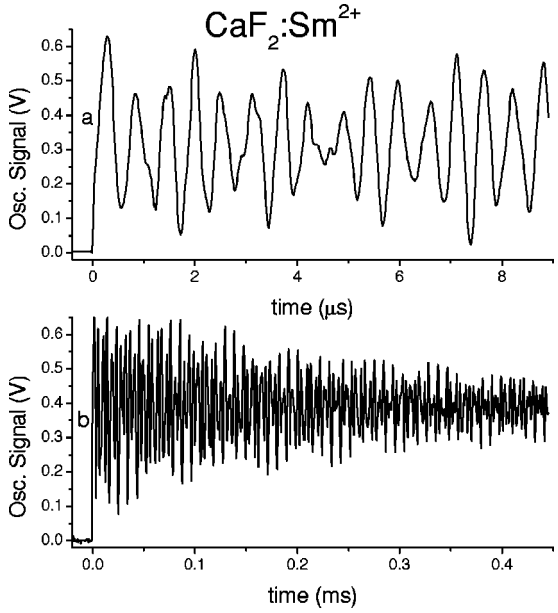

FIG. 4. Transient dielectric response of $CaF_2:Sm$ (No. 1) crystal on laser pulses of green ($\lambda=532$ nm) light of ~ 1 mJ energy for two different time intervals from the beginning of the laser pulse: (a) $t=0$ to 9 μs and (b) $t=0$ to 0.45 ms.

IV. EXPERIMENTAL RESULTS

Figures 3 and 4, on different time-scales, show oscilloscopic traces of signals registered with the mixer for $CaF_2:Sm$ (No. 1) crystal, see Table I, upon excitation with the frequency doubled or tripled Nd:YAG laser pulses. Both laser beams [green ($\lambda=532$ nm) and UV ($\lambda=355$ nm)] were collinear and equalized in intensity, and the phase of microwaves in the reference arm was not changed when switching measurements from green to UV light. It is important to note, that this sample has approximately the same transmission $\sim 50\%$ for both UV and green light, thereby the distribution of light energy absorbed in the crystal, was approximately identical for these laser beams. In both cases, the same prolonged oscillations of the signal with a period of about 0.6 μsec were observed. The oscillations of the signal are accompanied by beatings, probably, due to superposition of two or more simple harmonic modes with close frequencies and rather long decay time, ~ 1 msec, see Fig. 4. These oscillations are imposed on a sawtooth base signal which ''jumps'' at a laser pulse and slowly decays, but for a much longer time of 100 ms, just to the next laser pulse.

There is only one difference between the oscilloscopic traces of Figs. 3(a) and 3(b). Upon excitation by UV light, an additional ''peak'' was observed at ''starting'' time $t\sim 0$. Further on, we will refer to such peaks as the ''electronic'' signals, and the sawtooth base signals, accompanied by oscillations as the ''heating'' signals. (Detailed discussion of the nature of both signals is given in Sec. V). The heating signals appeared to be linearly dependent on the intensity I of laser light and were observed in all crystals studied. The oscillation parameters of the heating signal depend on the host crystal and on the size and the shape of the sample, see Fig. 5. The study shows that the heating signals are only seen in the dispersion mode and that the electronic peaks may be seen in any mode depending on the crystal.

In $CaF_2:Sm$ (No. 1) the electronic signals have comparable intensities in both absorption and dispersion modes. Their intensity dependence versus laser power is sublinear ($S^{el}\sim I^x$, where $x<1$). This results in predominance of the electronic signal, relatively to the heating signal, at small light intensities, see Fig. 3(a). The study of $CaF_2:Sm$ (No. 1) crystal upon excitation by tunable pumped dye laser revealed the fact that the electronic signal in this crystal exists only under light excitations with wavelength $\lambda<380$ nm.

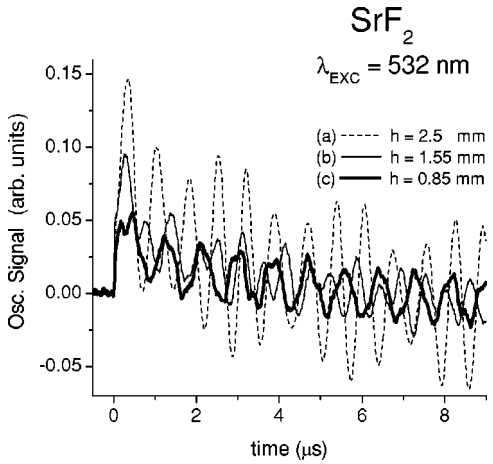

FIG. 5. Transient heating signals of doped SrF_2 crystals of the same diameter $d=2.5$ mm but different heights h after laser pulses of green ($\lambda=532$ nm) light. (a) $SrF_2:Tm$, $h=2.5$ mm; (b) $SrF_2:Sm$ (No. 2), $h=1.55$ mm; (c) $SrF_2:Tm$, $h=0.85$ mm. The signals are distorted due to the amplifier with the low bandpass frequency of ~ 1 MHz.

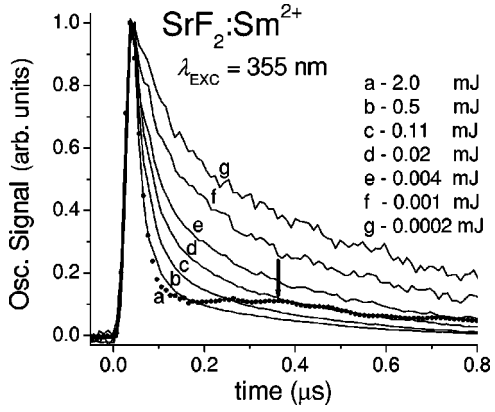

FIG. 6. (a) Normalized transient electronic signals of SrF_2:Sm (No. 1) crystal after laser pulses of UV ($\lambda = 355$ nm) light of different energy: (a) -2 mJ, (b) -0.5 mJ, (c) -0.11 mJ, (d) -0.02 mJ, (e) -0.004 mJ, (f) -0.001 mJ, and (g) -0.0002 mJ. The arrow shows the heating signal seen only on the curve (a).

A strong electronic signal was observed in the most concentrated SrF_2:Sm (0.21 mol. %) crystal upon excitation with either UV or green light. The heating signal (which is much weaker) appears only at the highest intensities of laser light. In this crystal the electronic signal is seen only in dispersion mode. It should be noted that the electronic peak has a considerable width, up to about 0.2 μsec and more at weak light intensities. Figure 6 shows that it narrows to about 50 ns at high light intensities, while Fig. 7 shows that its wings expand up to about 200 μsec and more after the laser pulse. The dependence of the electronic signal amplitude on the energy of the light pulses is approximately linear for extremely weak light, but has a square-root dependence ($S^{el} \sim \sqrt{I}$) at high light intensities, see Fig. 8. Due to the narrowing of the electronic peak, the ratio of the intensities of the electronic signal at its maximum and at its wings (for

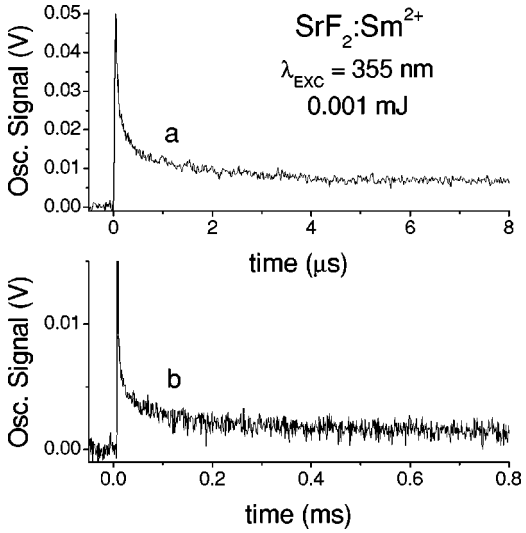

FIG. 7. Transient electronic signals of SrF_2:Sm (No. 1) crystal on laser pulses of UV ($\lambda = 355$ nm) light of ~ 0.001 mJ energy for two different time intervals from the beginning of the laser pulse: (a) $t = 0$ to 8 μs and (b) $t = 0$ to 0.8 ms.

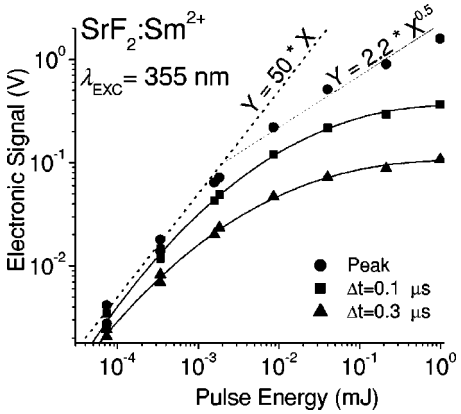

FIG. 8. Experimental (dots), interpolating (solid lines), and extrapolating linear (dot line) and square-root-law (dash line) dependences of the intensity of electronic signal versus the energy of laser pulses of UV ($\lambda = 355$ nm) light for SrF_2:Sm (No. 1) crystal. (●) Peak intensities, (■,▲) intensities measured with delay of (■) 0.1 μsec and (▲) 0.3 μsec after a laser pulse.

signal measured with delay of 0.1 μsec or 0.3 μsec after the laser pulse, see Fig. 8) increases with the intensity of the laser light. The dependence of the electronic signal amplitude on the wavelength of laser light in the range from 460 to 670 nm is presented in Fig. 9.

The well-defined sublinear dependence of the electronic signal amplitude versus the laser light intensity was observed for all Sm- or Tm-doped fluorite-type crystals studied.

In contrast, for CaF_2:Eu, a superlinear dependence, $S^{el} \sim I^{1.5}$, was found. In addition, the electronic peak was seen only in absorption mode. Therefore, by readjusting the phase-shifter in the reference arm of the setup, it was possible to single out either the heating signal or the electronic peak. In Fig. 10, the oscilloscopic traces observed either in dispersion or absorption mode are shown for low (0.2 mJ) and high (1 mJ) energies of UV laser pulses.

Unexpectedly strong electronic signals were observed upon excitation of SrF_2:Eu (0.5%) crystal by pulses of green

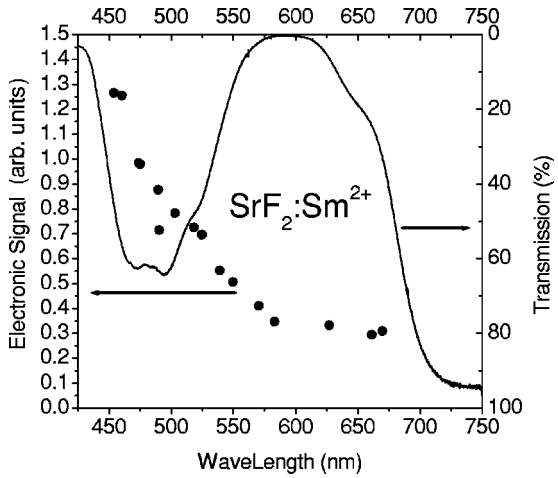

FIG. 9. Wavelength dependence of the amplitude of electronic signal (dots) and transmission spectrum (solid line) of SrF_2:Sm (No. 1) crystal.

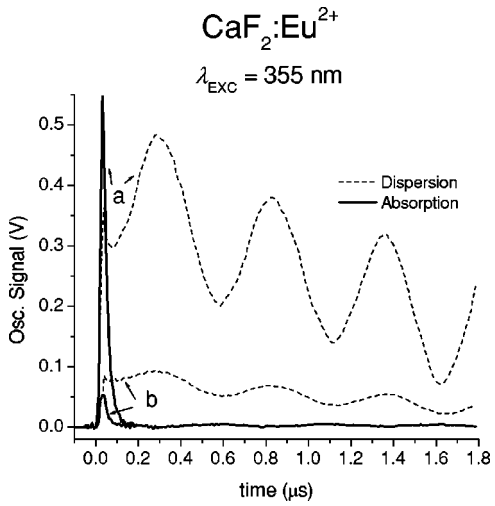

FIG. 10. Transient dielectric response of CaF_2:Eu crystal on laser pulses of UV ($\lambda = 355$ nm) light of (a) 1 mJ and (b) 0.2 mJ energy. The phase of microwaves in the reference arm was tuned to dispersion (dash line) and absorption (solid line) modes.

light in the range of its optical transparency, where absorption coefficient $k < 0.05\ \mathrm{cm}^{-1}$, see Fig. 11. The effect is observed in a wide spectral range from $\lambda = 460$ nm up to 620 nm (Fig. 12) and tends to saturate as the light intensity increases (Fig. 13). The time response of the signals in dispersion and absorption modes following a laser pulse appeared to be different, see Fig. 11. The signal registered in dispersion mode rises and reaches its maximum value during the laser pulse. The signal in absorption mode grows much more slowly. The dispersion signal completely decays in about 0.5 ms, i.e., approximately an order of magnitude faster than the absorption signal does (5 ms).

Upon excitation of LSO:Ce^{3+} crystal by laser pulses of UV light, the electronic peak is clearly seen, but the heating

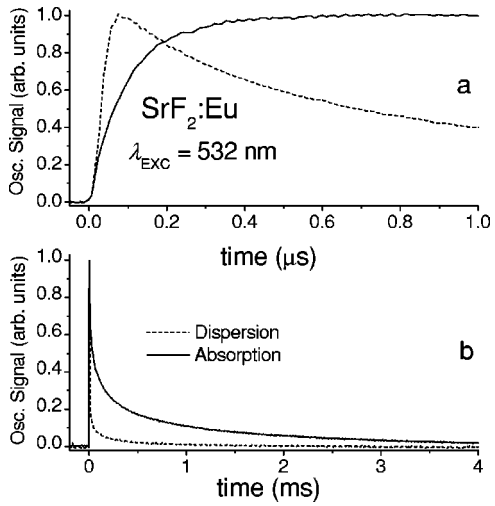

FIG. 11. Transient dielectric responses of SrF_2:Eu (0.5 mol. %) crystal on laser pulses of green ($\lambda = 532$ nm) light measured in absorption (solid line) and dispersion (dash line) modes for two different time intervals from the beginning of the laser pulse: (a) $t = 0$ to 1 μs and (b) $t = 0$ to 4 ms.

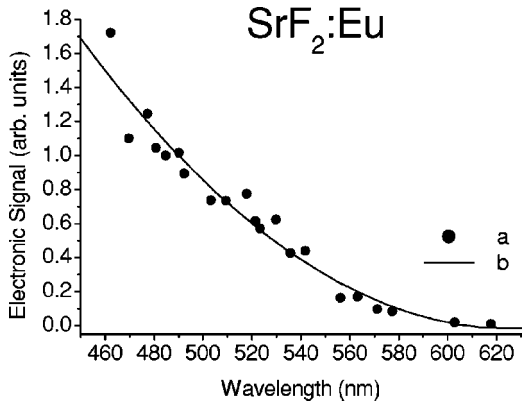

FIG. 12. (a) Wavelength dependence of the amplitude of transient electronic signal for SrF_2:Eu(0.5 mol. %) crystal. (b) Interpolation of the experimental dependence.

signal is nearly missing, see Fig. 14(a). This electronic peak of about 100 ns in width reveals itself only in the absorption mode. Its shape does not vary and its amplitude declines linearly with decreasing energy of the UV pulses by two orders of magnitude from 1 to 0.01 mJ. A study of its spectral dependence in the range from 532 to 275 nm has shown that the electronic signal appears upon illumination of the crystal by light of any wavelength in the range of its absorption spectrum [$\lambda < 410$ nm (3.1 eV)],[24] with an intensity that reproduces quite well the photoconductivity spectrum obtained by conventional technique.[12] Upon irradiation by green light ($\lambda = 532$ nm), only a very weak heating signal is observed at the highest light intensities.

Wave forms recorded for YAG:Ce^{3+} crystal are shown in Figs. 14(b) and 14(c). The microwave phase in the reference arm was tuned to the maximum intensity of the signals. Here, the heating signals were observed only under 355 nm laser excitation.

The experimental data for all crystals investigated by excitation with the second and third harmonics of Nd:YAG laser are presented in Table I. The data on the content of RE

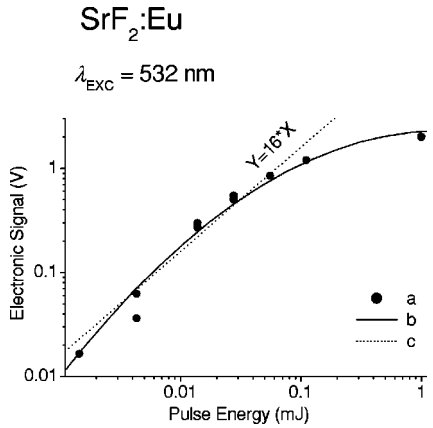

FIG. 13. SrF_2:Eu(0.5 mol. %) crystal. (a) Amplitude of the transient electronic signal versus energy of laser pulses of green ($\lambda = 532$ nm) light (dots). (b) Interpolation of the experimental dependence (solid line). (c) Extrapolating linear dependence (dash line).

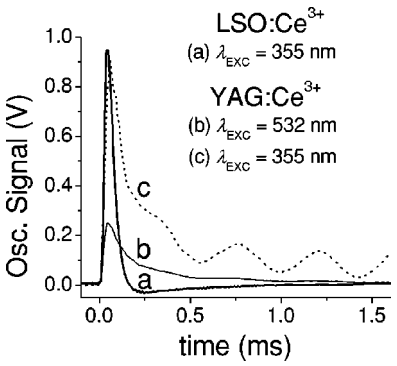

FIG. 14. Transient dielectric responses of (a) LSO:Ce^{3+} and (b,c) YAG:Ce^{3+} crystals on laser pulses of (a),(c) UV ($\lambda = 355$ nm) and (b) green ($\lambda = 532$ nm) light of energy of (a) 0.5 mJ and (b),(c) 1 mJ. The phase of microwaves in the reference arm was tuned to the maximum amplitude of the signals. The ''negative kick'' at 0.25 μsec is due to the distortion of the signal caused by bandpass limits (1–100 MHz) of the amplifier.

ions, on the evaluation of RE^{2+} concentration as well as the absorption coefficients, k, for exciting light with wavelengths of 532 and 355 nm are also given. The amplitudes of electronic S^{el} and heating S^{ht} signals were collected from various measurements and, if necessary, were recalculated to an incident energy of 1 mJ per pulse. Estimates of the ratio $S^{el}_{abs}/S^{el}_{dis}$ for some crystals are also presented in Table I to show the fractions of electronic signals observed in the absorption and the dispersion modes, as revealed by square-law detector studies (it was defined that $S^{el}_{abs}+S^{el}_{dis}=1$). It should be noted that the amplitude of the recorded signals depends strongly on the position of the sample in the resonator and on focusing practice of the laser beam at the surface of the sample. In addition, the investigated crystals had different dielectric losses and were of different optical quality. All these explains a significant error, $\pm 50\%$, in determination of absolute values of S^{el} and S^{ht} given in Table I.

V. DISCUSSION OF RESULTS

A. Electronic signal

The narrow electronic peaks observed on the oscilloscope as transient dielectric responses of rare-earth-doped crystals on irradiation by pulses of laser light [see Figs. 3(a), 6, 7, 10, and 14] obviously correspond to the RE activator ion photoionization and to the presence of released electrons in the conduction band of the host following absorption of light into the $4f^{n-1}5d$ electronic states of the involved RE ions. Thus, the rising front of these electronic peaks is due to the photoionization process which proceeds as follows:[22,25–26]

$$RE^{2+}+\hbar\omega \Rightarrow RE^{3+}+e, \tag{16a}$$

for divalent ions of Sm, Eu and Tm, and

$$Ce^{3+}+\hbar\omega \Rightarrow Ce^{4+}+e, \tag{16b}$$

for the trivalent Ce ion. Decay of the electronic signal starts on completion of the laser pulse, when the reverse process to Eq. (16) is carried out, and the electrons, that were released into the conduction band, recombine with trivalent RE ions of Sm, Eu, and Tm

$$RE^{3+}+e \Rightarrow RE^{2+} \tag{17a}$$

or with tetravalent Ce ion

$$Ce^{4+}+e \Rightarrow Ce^{3+}. \tag{17b}$$

Thus, the initial charging state of impurities is restored.

The most clear results were obtained with the LSO:Ce^{3+} crystal, see Fig. 14(a). The electronic peak linearly depends on the intensity of the UV laser pulses. It is a ''pure'' signal of microwave absorption. Thus, photoionization of the Ce^{3+} impurity in LSO:Ce^{3+} results in the occurrence of dielectric losses which can be explained by electronic conductivity arising in the crystal due to laser pulses. The estimated lifetime of electrons in the conduction band of LSO is $\tau_{el} \approx 100$ ns. The electronic signal appears upon illumination of LSO:Ce^{3+} by light of any wavelength in the range of the $4f \rightarrow 5d$ absorption spectrum of Ce^{3+} ions. Its wavelength dependence is in perfect agreement with the room-temperature photoconductivity spectrum obtained earlier by the conventional method of photocurrent measurement.[12]

In CaF_2:Eu, the observed electronic peak is also a ''pure'' signal of microwave absorption. The estimated lifetime of electrons in the conduction band of CaF_2:Eu is $\tau_{el} \approx 40$ ns. Now, the 355 nm wavelength of the laser corresponds approximately to the center of the first $4f^7 \rightarrow 4f^6 5d$ absorption band,[4,27] and the intensity of the electronic peak versus laser intensity shows that S^{el} increases as $I^{1.5}$. As the probability of excitation of a system by a two-step process depends on the light intensity as the power law I^x, where x can vary from 1 to 2 depending on the parameters of the system,[28] this superlinear dependence, apparently, shows that two quanta of UV light are required for the photoionization of Eu^{2+} ions in CaF_2:Eu. This can be called an excited-state photoionization. The first absorbed quantum excites this divalent ion into the $4f^6 5d(e_g)$ manifold of the $4f^6 5d$ configuration and then the second quantum may bring an electron into the conduction band. It is not surprising that, under 355 nm (3.5 eV) irradiation, two quanta are needed for the photoionization of Eu^{2+} ions in CaF_2:Eu because conventional photocurrent measurements indicated that the photoconductivity threshold is located at 3.8 eV (326 nm) in this crystal.[4] Moreover, efficient excited-state absorption from the lowest localized $4f^6 5d$ states of Eu^{2+} in CaF_2:Eu has been found by means of the pump-probe technique and interpreted as transition from these $4f^6 5d(e_g)$ states to the conduction band.[27]

The dielectric responses of YAG:Ce^{3+} crystal on pulses of UV light are rather similar to those observed for doped fluorite-type crystals, see Fig. 14(c). There is a strong electronic signal and a heating signal accompanied by its characteristic oscillations with a period of about 0.7 μsec. The lifetime of an electron in the conduction band proved to be ~ 100 ns. An unexpected thing was the observation of an electronic signal upon excitation by pulses of green light at the long-wavelength edge of the $4f \rightarrow 5d$ absorption transition of Ce^{3+} ions,[29] see Fig. 14(b). At such excitation the

heating signal is nearly missing, because of very weak absorption of green light, see Table I. Thus, the photoionization efficiency under green light excitation appeared to be much higher than that of UV light by an order of magnitude. As in the case of CaF_2:Eu^{2+}, such electronic signal is also supposedly due to a two-step photoionization. Indeed, the proposed energy level diagram for Ce^{3+} in YAG:Ce indicates that the absorption of two quanta of green (532 nm) light may bring Ce^{3+} electron up into the conduction band.[29]

The electronic peak is clearly present in the dielectric responses of CaF_2:Sm crystals on pulses of UV light, but absent when laser pulses of green light of the same energy are applied, compare Figs. 3(a) and 3(b). Our study has shown that the photoexcitation of electrons in the conduction band of CaF_2:Sm can only be realized by light with $\lambda < 380$ nm. Thus obtained, the threshold energy of the photoionization process for Sm^{2+} ions in CaF_2, 3.3 eV, significantly exceeds the edge of the $4f^6 \rightarrow 4f^5 5d$ absorption band which is located at 1.8 eV.[4] The threshold value found here does not confirm the photoconductivity spectrum presented in Ref. 4, but is close enough to the theoretical value (3.6 eV) calculated in the same paper. In SrF_2:Sm crystals the photoionization of Sm^{2+} ions is possible upon light excitation in the whole range of $4f^6 \rightarrow 4f^5 5d$ absorption spectrum of these ions. However, Fig. 9 shows that the efficiency of this process grows with an increase in the excitation energy from the long-wave edge of the absorption band ($\lambda = 700$ nm). The photoexcitation of electrons into the conduction band by green light is possible in all fluorite-type crystals, doped with Tm^{2+} ions (see Table I). It can be stated, that the process of photoionization of both Sm^{2+} and Tm^{2+} ions requires only one quantum of light for its realization. This follows from the linear dependence of the electronic signal amplitude versus the excitation intensity for extremely weak light flows, see Fig. 8.

The unexpected result of our study is the sublinear dependence of the amplitude of the electronic peak and its noticeable narrowing with an increase in energy of laser pulses for all investigated fluorite-type crystals activated by Sm^{2+} and Tm^{2+} ions. Let us examine the results obtained for CaF_2:Sm crystal, see Fig. 3(a). The amplitude of heating signals is proportional to the energy of light absorbed by the crystal, and because of that, linearly increases with an increase in energy of laser pulses. On the contrary, the amplitude of the electronic peak is saturated by increasing intensity of light. The nonlinear phenomena are also clearly seen in SrF_2:Sm (No. 1), see Fig. 8. Moreover, for this crystal the lifetime of electrons in the conduction band appears to increase significantly, from 50 to 200 ns and more (see Fig. 6) by decreasing the intensity of laser light from 2 to 2×10^{-4} mJ. These phenomena cannot be explained by saturation of absorption in these crystals or their heating by powerful laser pulses. Indeed, the sample warming at the highest intensity of laser light did not exceed 20 K, see Sec. V B. And depopulation of the ground state of RE ions after laser pulses did not exceed 10% of the total concentration of the involved RE ions. At this stage, it is interesting to note that the change in the dependence of the photoconductivity on the light intensity from linear to square-root law with increasing intensity of light, see Fig. 8, is characteristic of noncrystalline (semiconducting) materials.[30] There, the recombination mechanism of excess (photoexcited) carriers changes from monomolecular to bimolecular with an increase in their photogeneration rate. In our case, however, the nonlinear phenomena observed, probably, testify to the fact that electrons, released into the conduction band as a result of photoionization of RE impurity in accordance with Eq. (16a) are not free, but appear to be bound, captured by traps with their energy levels being well below the ''mobility edge.''[30] From the traps they can be thermally evaporated back into the conduction band. It is reasonable to assume, that the bound electrons do not participate in the recombination process of Eq. (17a), and their thermal excitation to the conduction band requires some time which depends on the depth of the trap (deep or shallow). The lifetime of carriers bound on traps, probably, also determines the decay time of the electronic signal after the pulses of laser light. With increasing the energy of laser pulses, the total concentration of electrons released into the conduction band is also increasing and the deep traps are gradually filled. From the shallow traps, the electrons are easily freeing, recombining fast with the trivalent RE ions in accordance with Eq. (17a).

These suppositions about bound electrons also allow us to explain the fact that in fluorite-type crystals the electronic signal usually has appreciable contribution of dispersion mode. The most interesting case is SrF_2:Sm^{2+} (No. 1) crystal, where the dielectric response is only observed in the dispersion mode. Here, the photoexcitation of electrons into the conduction band results only in an increase of polarizability of the crystal, but not in photoconductivity. The electrons appear to be limited in their movement space, probably, captured by traps. From the value of an electronic dispersion signal ($S_{\mathrm{dis}}^{\mathrm{el}} = 1.5$ V recorded upon illumination by pulses of UV laser light with energy of 1 mJ), it is possible to get a lower estimate of the increase $\Delta\alpha_{\mathrm{bound}}$ of the sample polarizability due to these bound electrons:

$$\Delta\alpha_{\mathrm{bound}} \geqslant \Delta\varepsilon_1 V_s \Big/ 4\pi \frac{\varepsilon_1 + 2}{3} n_{\mathrm{ph}} \sim 10^{-23} \ \mathrm{cm}^3, \quad (18)$$

if we assume that Θ, the quantum efficiency of photoionization process, is equal to unity (see Sec. II). It should be noted, that because of sublinear dependence of the electronic signal on the intensity of the excitation light, see Fig. 8, the estimate has to be, in fact, by one or two orders of magnitude higher than that given by Eq. (18). On the basis of this estimate and the fact that, certainly, $\Theta < 1$, it is possible to expect, that the radius of the orbit of an electron bound to a trap covers a few lattice constants.

Such electron traps could be formed by extended defects in a crystal lattice. It is also possible that the traps are formed by clusters or cluster ''grains'' which exist in fluorite-type crystals doped with RE ions in concentration of 0.1 mol. % or more.[31,32] These impurity clusters, appear to contain only trivalent and not ''photoactive'' divalent RE ions which are supposed to form the simple cubic centers statistically distributed in the fluorite crystal lattice.[9,31,33] It is interesting to note that electronic traps appear to be absent, and photo-

excited electrons to be free, if there are no clusters, as one can assume for CaF_2 doped with Eu ions in low concentration of 0.01 mol. %. Note that the electronic signal in the latter crystal is seen only in the absorption mode, see Table I.

In SrF_2:Eu (0.5 mol. %) irradiated by pulses of green light in the optical ''transparency'' range of the crystal, a strong electronic signal is present in the dispersion mode, see Fig. 11(a) and Table I. The appropriate estimates of polarizability of the photoexcited bound electron in this case give a ''gigantic'' value of $\Delta\alpha_{\text{bound}} \geqslant 10^{-19}$ cm^3. Upon termination of a laser pulse, the signal in the dispersion mode starts to decay and that in the absorption mode is continuing to increase, see Fig. 11(a). Such behavior of the signal in the absorption mode, possibly, testifies to releasing of initially bound photoexcited electrons. It follows from Fig. 11(b) that, less than 1 ms after the laser pulse, the bound electrons disappear and only the free ones remain for a longer time of about a few ms. The effect exists in a wide spectral range of excitation light and saturates with an increase in intensity of light, see Figs. 12 and 13. All these facts, are probably evidence of complex color centers existing in SrF_2:Eu (0.5 mol. %) crystal in extremely small concentration. The observed signal in the dispersion mode, probably, corresponds to excitation of these centers into a metastable state by laser light, and the signal in the absorption mode to the subsequent (thermal) ionization of the centers and formation of the mobile charged particles (electrons). This process is convertible and its cycle lasts about 4 ms. Such complex color centers in fluorite-type crystals doped with europium ions were unknown before. However, rare-earth-associated color centers that show large photochromic effects were found in CaF_2 doped with La, Ce, Gd, or Tb.[26] Thus far, one could not exclude the possible formation of similar aggregates in SrF_2:Eu.

B. Heating signal

It is natural to ascribe the saw-tooth signal (that arises at the moment of action of a laser light and that is accompanied by oscillations persisting a long time after the termination of a laser pulse, see Figs. 4 and 5) to the process of dissipation of laser energy absorbed in the volume V_S of a crystal. Indeed, during the short laser pulse, the absorbed light energy causes a ''thermal impact''—''instant'' warming up of the crystal. However, the corresponding thermal expansion of a sample develops with the propagation velocity of elastic waves, i.e., it goes relatively slowly and persists after the laser pulse. The stored light energy causes crystal vibrations accompanied by a change in its form and local changes in its dielectric constant. These periodic oscillations of the parameters of the crystal placed in the microwave resonator induce the oscillating heating signals in the measuring arm.

Since the dielectric constant of a substance is a function of temperature, the ''instant'' warming of a sample during the action of a laser pulse results in a steplike change in its dielectric constant, which may be observed as the corresponding steplike signal in dielectric response of the sample recorded in dispersion mode. In a stationary regime of a periodic chain of laser pulses, the dielectric constant returns to some definite value at the start of each successing laser pulse. On the whole, the observable heating signal has a sawtooth shape with a period equal to that of the chain of laser pulses (10 Hz), on which the oscillations caused by elastic vibrations of the crystal after each laser pulse are imposed. Measurements show that the heating signals are seen only in the dispersion mode. This fact is in accord with the above suggestions about the special role which the dielectric constant and its temperature dependence play in formation of the heating signal.

It is interesting to note, that an ''instant'' heating of a ''standard'' fluorite-type crystal which absorbed the energy $\Xi = 1$ mJ of a single laser pulse does not exceed

$$\Delta T = \frac{\Xi M_s}{\rho_s V_s c_P} < 0.03 \text{ K}, \tag{19}$$

in which M_s is the molecular weight of the crystal, ρ_s is its density, and c_P its heat capacity. From the value of ΔT found and the temperature dependence of the dielectric constant,[15] it follows that the expected value of the amplitude of the sawtooth heating signal is equal to $S_{\text{dis}}^{\text{ht}} \sim 0.3$ V, in accordance with the experimental data of Table I by an order of magnitude. The experimental estimates of the time of establishment of the sample temperature, see Sec. III, lead to the conclusion that the average temperature of the crystal irradiated by a periodic chain of laser pulses raises much more, up to 20 K.

Let us look at elastic vibrations of a crystal in details. The equation for elastic vibrations is[15]

$$\rho_s \frac{d^2\vec{\rho}}{dt^2} = (c_{11} - c_{12} - 2c_{44}) \left[\frac{\partial^2 u}{\partial x^2}\vec{i} + \frac{\partial^2 v}{\partial y^2}\vec{j} + \frac{\partial^2 w}{\partial z^2}\vec{k} \right] + (c_{12} + 2c_{44}) \text{grad div}\,\vec{\rho} - c_{44}\,\text{rot rot}\,\vec{\rho}, \tag{20}$$

where $\vec{\rho} = u\vec{i} + v\vec{j} + w\vec{k}$ is the displacement vector and c_{11}, c_{12}, and c_{44} are the elastic constants. If the condition of elastic isotropy $c_{11} - c_{12} = 2c_{44}$ (Ref. 15) is satisfied, one longitudinal stretching wave and two transverse shear waves should spread in the crystal. The speed of the waves does not depend on a propagation direction.

In our experiments the elastic waves were excited by pulses of laser light in cylindrical samples having rather moderate absorption coefficient values. This fact allows us to assume nearly uniform instant warming of a sample in all its volume during the laser pulse. Under condition of elastic isotropy, mainly the longitudinal waves should be excited in this case. For longitudinal waves $\text{rot}\,\vec{\rho} = 0$. After the replacement $\vec{\rho} = -\text{grad}\,\varphi$,[34] Eq. (20) transforms into the well known wave equation[10]

$$\rho_s \frac{d^2\varphi}{dt^2} = (c_{12} + 2c_{44})\Delta\varphi. \tag{21}$$

For the cylindrical samples studied, the most interesting vibration modes are the three with the lowest frequencies.

(a) Vibrations of L_{01} type, axial stretching mode (stretching along the axis of a cylindrical sample). The wave equa-

TABLE II. Anisotropy factor and velocities of elastic waves in fluorite-type crystals.

	CaF_2	SrF_2	BaF_2
$2c_{44}/(c_{11}-c_{12})$,[a] (10^{11} dynes/cm^2)	0.562	0.778	1.211
$\sqrt{c_{11}/\rho_0}$,[a] (10^5 cm/s)	7.177	5.459	4.085
$\sqrt{c_{44}/\rho_0}$,[a] (10^5 cm/s)	3.249	2.747	2.273
$\sqrt{(c_{12}+2c_{44})/\rho_0}$,[a] ($10^5$ cm/s)	5.920	5.048	4.300
v_L, (10^5 cm/s)	5.9 ± 0.1[b]	4.7 ± 0.2[b] 5.3 ± 0.3[c]	3.9 ± 0.3[b]

[a]Elastic constants are from Ref. 33.

[b]Calculated values from the experimental data of this work for the samples with $h=1.5$–2.5 mm.

[c]Calculated values from the experimental data of this work for the sample with $h=0.8$ mm.

tion solution is $\varphi_{01}\sim\sin[(\pi/h)z]$. The amplitude of the sample vibrations is $\vec{\rho}\sim\cos[(\pi/h)z](\vec{z}/z)$ and the period is $T_{01}=2h/v_L$.

(b) Vibrations of L_{10} type, radial stretching mode (stretching along the radius of a cylindrical sample). The wave equation solution is $\varphi_{10}\sim J_0(k_c r)$. The amplitude of vibrations is $\vec{\rho}=\vec{\rho}(r)\sim J_1(k_c r)(\vec{r}/r)$ and the period is $T_{10}=(\pi/1.841)(d/v_L)$.

(c) Vibrations of L_{11} type, ''breathing'' mode. The wave equation solution is $\varphi_{11}\sim J_0(k_c r)\sin[(\pi/h)z]$. The amplitude of vibrations is $\vec{\rho}\sim -k_c J_1(k_c r)\sin[(\pi/h)z](\vec{r}/r)+(\pi/h)J_0(k_c r)\cos[(\pi/h)z](\vec{z}/z)$ and the period is $T_{11}=(d/v_L)/\sqrt{(1.841/\pi)^2+(d/2h)^2}$. Here, v_L is the velocity of a longitudinal wave, $k_c(d/2)=1.841$ is the first root of the equation $(d/dx)J_1(x)=0$, J_0 and J_1 are Bessel functions of the first kind, $0\leqslant z\leqslant h$, and $0\leqslant r\leqslant d/2$.

The oscillations of heating signals, observed in all the fluorite-type crystals studied can be ascribed to the dominant contribution of L_{11} ''breathing'' mode. The experimental period values of the strongest oscillations are equal to $T_{11}=0.56\pm0.01$ μs for several doped CaF_2 samples of $h\approx2.5$ mm height. The period T_{11} is equal to 0.70 ± 0.02 and 0.55 ± 0.02 μs for SrF_2 samples of $h\approx2.5$ and 1.55 mm, respectively, and 0.83 ± 0.04 μs for the BaF_2 sample of $h\approx2.5$ mm. These values do not depend on the type of RE activator ions in the crystals. In a thin disc of SrF_2:Tm of $h\approx0.8$ mm, two different vibrational modes with different periods were observed. We identify these as the L_{11} mode with $T_{11}=0.28\pm0.02$ μs and the L_{10} mode with $T_{10}=0.85\pm0.02$ μs. These data made it possible to estimate the propagation velocities of longitudinal waves in the CaF_2, SrF_2, and BaF_2 crystals studied. They are listed in Table II together with other parameters taken and calculated from Ref. 33. With an accuracy of $\pm10\%$ the estimated velocity values are in agreement with the theoretical values of $v_L=\sqrt{(c_{12}+2c_{44})/\rho_0}$ defined by Eq. (21), see Table II.

It should be noted, that because of the specific focusing details of the laser beam on the sample surface and the absorption of laser light inside the samples, warming under pulses of laser light was not uniform throughout the volume of the samples. Therefore, the excitation of shear elastic waves was also possible. The increase in number of active vibration modes, seems to be capable of explaining the existence of two or several elastic waves with close frequencies that form beats in the oscillatory heating signals, see Fig. 4 and 5. The shear waves have also to be considered because of the fact that in cubic fluorite-type crystals the anisotropy factor $A=2c_{44}/(c_{11}-c_{12})$ is not unity, as it should be for elastic isotropy, see Table II. In this case, the division of elastic waves into longitudinal and transverse modes is only possible for propagation along the main crystallographic axes of the crystal.[15] For example, for elastic waves propagating in the [100] direction, the velocity of the shear and longitudinal waves is equal to $v_T=\sqrt{c_{44}/\rho_0}$ and $v_L=\sqrt{c_{11}/\rho_0}$, respectively. The experimental velocity values obtained in our work are between these two extremes, see Table II. Thus, the elastic vibrations (observed in our fluorite samples of a random crystallographic orientation) were of mixed (longitudinal-transverse) modes. For their exact description, obviously, it is necessary to find an exact solution of Eq. (20).

VI. CONCLUSIONS

An experimental technique based on the detection of the dielectric response of a rare-earth doped insulator placed into a microwave resonator and irradiated by pulses of laser light is offered to measure the rare-earth photoionization thresholds in doped dielectric crystals. This technique does not present higher sensitivity than the conventional method of photoconductivity measurements ''employing a condenser with blocking electrodes.'' However, it makes it possible to record the transients in the dielectric permittivity of doped crystals during and after the excitation light pulses and, thus, to study the photoconductivity process dynamics.

In dielectric fluorite-type crystals doped with divalent ions of Sm, Eu, and Tm, and also in oxide LSO and YAG crystals doped with trivalent Ce ions, sufficiently strong signals of electronic ''photoconductivity'' were observed upon photoexcitation of the rare-earth activator into $4f^{n-1}5d$ absorption bands. The electronic ''photoconductivity'' signal was usually observed on a background of an oscillating heating signal. The lifetime of photoexcited electrons in the conduction band of the dielectric crystals studied appears to vary from 40 up to 100 ns or more. In different crystals, the photoionization of RE impurity can provide both free and bound electrons. In the former case, the corresponding change in the dielectric loss factor ε_2 and in the latter the change in the dielectric constant ε_1 of the sample induces an electronic signal. The bound states of photoexcited electrons in fluorite-type crystals are obviously formed by electrons captured by traps. The sublinear growth of the amplitude of an electronic signal and decrease of the lifetime of photoexcited electrons with an increase in the intensity of laser pulses could be explained by filling deep traps. From shallow traps, the electrons are easily thermally evaporated into the conduction band and, after recombination with the cubic RE^{3+} centers, restore an initial charge state of RE impurities.

It is interesting to note that electronic traps appear to be absent, so that photoexcited electrons remain free, provided

there are no defect clusters. This is the case for CaF_2 doped with a low concentration (0.01 mol. %) of Eu ions. The photoconductivity of free electrons was also observed in LSO:Ce^{3+} crystal. The study of spectral dependences of electronic signals allows us to find the threshold values of the photoionization energy of RE ions. Such measurements were fulfilled for $CaF_2:Sm^{2+}$ and LSO:Ce^{3+} crystals indicating threshold values at 3.3 and 3.1 eV, respectively.

The change of dielectric permittivity per absorbed photon was found in SrF_2:Eu under laser pulses of VIS light in the ''transparency'' optical spectrum range of the crystal. The phenomenon is possibly due to photoactive color centers associated with Eu ions, which exist there in rather small concentration and have been unknown before.

Powerful laser pulses used in the experiments make it possible to observe photoionization of doped dielectric crystals via a two-step absorption process. Such excited-state photoionization was observed in $CaF_2:Eu^{2+}$ and, possibly, in YAG:Ce^{3+} crystals.

ACKNOWLEDGMENTS

We acknowledge the CNRS (Center National de la Recherche Scientifique) in France for the financial support given to S.A.K. in the LPCML (Laboratoire de Physico-Chimie des Matériaux Luminescents).

[1] C. Dujardin, C. Pédrini, J. C. Gâcon, A. G. Petrosyan, A. N. Belsky, and A. N. Vasiliev, J. Phys.: Condens. Matter **9**, 5229 (1997).
[2] C. W. Thiel, H. Cruguel, H. Wu, Y. Sun, G. J. Lapeyre, R. L. Cone, R. W. Equall, and R. M. Macfarlane, Phys. Rev. B **64**, 085107 (2001).
[3] C. Pédrini, D. S. McClure, and C. H. Anderson, J. Chem. Phys. **70**, 4959 (1979).
[4] C. Pédrini, F. Rogemond, and D. S. McClure, J. Appl. Phys. **59**, 1196 (1986).
[5] M.-F. Joubert, S. A. Kazanskii, Y. Guyot, J. C. Gâcon, J. Y. Rivoire, and C. Pédrini, Opt. Mater. (Amsterdam, Neth.) **24**, 137 (2003).
[6] S. Grabtchak and M. Cocivera, Phys. Rev. B **50**, 18 219 (1994); **58**, 4701 (1998).
[7] M. Ichimura, H. Tajiri, Y. Morita, N. Yamada, and A. Usami, Appl. Phys. Lett. **70**, 1745 (1997); M. Ichimura, N. Yamada, H. Tajiri, and E. Arai, J. Appl. Phys. **84**, 2727 (1998).
[8] S. V. Garnov, A. I. Ritus, S. M. Klementov, S. M. Pimenov, V. I. Konov, S. Gloor, W. Lüthy, and H. P. Weber, Appl. Phys. Lett. **74**, 1731 (1999).
[9] S. A. Kazanskii, D. S. Rumyantsev, and A. I. Ryskin, Phys. Rev. B **65**, 165214 (2002). In this paper, the filling factor η_E, was defined as the inverse value $\eta_E = \eta^{-1}$.
[10] C. P. Poole, *Electron Spin Resonance: A Comprehensive Treatise on Experimental Techniques* (Interscience, New York, 1966).
[11] M. Raukas, S. A. Basun, W. van Schaik, W. M. Yen, and U. Happek, Appl. Phys. Lett. **69**, 3300 (1996).
[12] W. M. Yen, M. Raukas, S. A. Basun, W. van Schaik, and U. Happek, J. Lumin. **69**, 287 (1996).
[13] G. Feher, Bell Syst. Tech. J. **36**, 449 (1957).
[14] D. R. Bosomworth, Phys. Rev. **157**, 709 (1967).
[15] C. Kittel, *Introduction to Solid State Physics* (Wiley, New York, 1957).
[16] B. Moine, B. Courtois, and C. Pédrini, J. Phys. (Paris) **50**, 2105 (1989).
[17] B. Moine, B. Courtois, and C. Pédrini, J. Lumin. **50**, 31 (1991).
[18] D. S. McClure and C. Pédrini, Phys. Rev. B **32**, 8465 (1985).
[19] The photosensitivity $\omega_0 \eta$ used in Ref. 4 is equal to $\tau_{el}(\Theta\mu)_{min}$ in our notations.
[20] Z. J. Kiss and P. N. Yocom, J. Chem. Phys. **41**, 1511 (1964).
[21] V. A. Arkhangelskaya, B. I. Maksakov, and P. P. Feofilov, Fiz. Tverd. Tela (Leningrad) **7**, 2260 (1965) [Sov. Phys. Solid State **7**, 1827 (1966)].
[22] V. A. Arkhangelskaya, M. N. Kiseleva, and V. M. Shraiber, Opt. Spectrosk. **23**, 509 (1967) [Opt. Spectrosc. **23**, 275 (1967)]
[23] Z. J. Kiss, Phys. Rev. **127**, 718 (1962).
[24] Y. Guyot, H. Loudyi, S. A. Kazanskii, J. C. Gâcon, C. Pédrini, and M.-F. Joubert, Rad. Meas. (to be published).
[25] B. Welber, J. Chem. Phys. **42**, 4262 (1965).
[26] B. W. Faughnan, D. L. Staebler, and Z. J. Kiss, Appl. Solid State Sci. **2**, 107 (1971).
[27] J. F. Owen, P. B. Dorain, and T. Kobayasi, J. Appl. Phys. **52**, 1216 (1981).
[28] M. R. Brown, W. A. Shand, and J. S. S. Whiting, Brit. J. Appl. Phys. **16**, 619 (1965); P. P. Feofilov, in *Physics of Impurity Centres in Crystals*, edited by G. S. Zavt (Academy of Sciences of the Estonian SSR, Tallin, USSR, 1972), p. 539.
[29] D. S. Hamilton, S. K. Gayen, G. J. Pogatshnik, R. D. Ghen, and W. J. Miniscalco, Phys. Rev. B **39**, 8807 (1989).
[30] N. F. Mott and E. A. Davis, *Electron Processes in Non-Crystalline Solids* (Clarendon Press, Oxford 1979), p. 260.
[31] M. P. Miller and J. C. Wright, J. Chem. Phys. **68**, 1548 (1978); Sun-II Mho and J. C. Wright, *ibid.* **81**, 1421 (1984).
[32] S. A. Kazanskii, Zh, Eksp. Teor. Fiz. **89**, 1258 (1985) [Sov. Phys. JETP **62**, 727 (1985)]; S. A. Kazanskii and A. I. Ryskin, Fiz. Tverd. Tela (St.Petersburg) **44**, 1356 (2002) [Sov. Phys. Solid State **44**, 1415 (2002)].
[33] *Crystals with the Fluorite Structure*, edited by W. Hayes (Clarendon Press, Oxford, 1974), p. 47.
[34] E. Madelung, *Die Mathematischen Hilfsmittel Des Physikers* (Springer-Verlag, Berlin, 1957).